

Constraints on non-thermal Dark Matter from PLANCK lensing extraction

L.A. Popa and A. Vasile §

ISS Institute for Space Sciences Bucharest-Magurele, Ro-76900 Romania

E-mail: lpopa@venus.nipne.ro and avasile@venus.nipne.ro

Abstract. Distortions of CMB temperature and polarization anisotropy maps caused by gravitational lensing, observable with high angular resolution and sensitivity, can be used to constrain the sterile neutrino mass, offering several advantages against the analysis based on the combination of CMB, LSS and Ly α forest power spectra. As the gravitational lensing effect depends on the matter distribution, no assumption on light-to-mass bias is required. In addition, unlike the galaxy clustering and Ly α forest power spectra, the projected gravitational potential power spectrum probes a larger range of angular scales, the non-linear corrections being required only at very small scales.

Taking into account the changes in the time-temperature relation of the primordial plasma and the modification of the neutrino thermal potential, we compute the projected gravitational potential power spectrum and its correlation with the temperature in the presence of DM sterile neutrino.

We show that the cosmological parameters are generally not biased when DM sterile neutrino is included. From this analysis we found a lower limit on DM sterile neutrino mass $m_{\nu_s} > 2.08$ keV at 95% CL, consistent with the lower mass limit obtained from the combined analysis of CMB, SDSS 3D power spectrum and SDSS Ly α forest power spectrum ($m_{\nu_s} > 1.7$ keV).

We conclude that although the information that can be obtained from lensing extraction is rather limited due to the high level of the lensing noise of PLANCK experiment, weak lensing of CMB offers a valuable alternative to constrain the dark matter sterile neutrino mass.

PACS numbers: CMBR theory, dark matter, cosmological neutrinos

§ To whom correspondence should be addressed: lpopa@venus.nipne.ro

Introduction

The latest results of the cosmic microwave background (CMB) temperature and polarization anisotropies from WMAP 3-year observations [1, 2] combined with other tracers such as large-scale structure (LSS) galaxy surveys, supernovae luminosity distance and Ly α forest, have lead in specifying the Λ CDM model as the cosmological concordance model [3, 4].

The direct confirmation of the Λ CDM theory is the detection of the acoustic Doppler peaks structure of the CMB angular power spectrum. Further successes are related to the correct prediction of the hierarchical structure formation via gravitational instability, the abundance of clusters at small redshifts, the spatial distribution and the number density of galaxies, the LSS matter power spectrum, the Ly α forest amplitude and spectrum [5]. Despite its successes on large scales, the Λ CDM model produces too much power on small scales. In general, the observed structures have softer cores, lower concentrations and are less clumped than those predicted by the Λ CDM model (see Ref. [6] and references therein).

A possibility to alleviate the accumulating contradiction between the Λ CDM model predictions on small scales and the observations is to add properties to the dark matter (DM) sector, relaxing the hypothesis on dark matter as being cold. Free streaming due to the thermal motion of the DM particles is the simplest known mechanism for smearing out small scale structure. Between the large free streaming distance of Hot Dark Matter (HDM) particles and the small free streaming distance of Cold Dark Matter (CDM) particles lies the intermediate scale of Warm Dark Matter (WDM) particles [7, 8]. The velocity dispersion of WDM particles is sufficient to alleviate some contradictions between the Λ CDM model predictions and observations such as: the predicted number of halos compared with the observed number of satellite galaxies in the Local Group [8, 9], the prediction of $1/r^\alpha$ ($1 < \alpha < 1.2$) behavior for galaxy rotation curves compared with the observed linearly rising behavior [10, 11, 12], the prediction of too much baryonic material with low angular momentum to form the observed rotationally disk galaxies [13].

On the other hand, in addition to the evidence for mixing of active neutrinos from solar and atmospheric oscillation experiments, there are indications for another oscillation with larger mass-squared difference coming from short base-line neutrino oscillation experiments [14, 15] that can be explained by adding one or two sterile neutrinos with eV-scale mass to the standard scheme with three active neutrinos (see Ref.[16] for a recent analysis).

Such results have impact on cosmology because sterile neutrinos can contribute to the number of relativistic degrees of freedom at the Big Bang nucleosynthesis [17]. These models are subject to strong bounds on the sum of active neutrino masses from the combination of various cosmological data sets [18, 20] that rule out a thermalized sterile neutrino component with eV mass-scale [4, 19].

However, there is the possibility to accommodate the cosmological observations with

data from short base-line neutrino oscillation experiments by postulating that sterile neutrino is not thermalized and has a phase-space distribution significantly suppressed relative to the thermal distribution. It is already known that sterile neutrino with mass of few keV - the Tremaine-Gunn [21] bound - provides a valuable DM candidate [22, 23, 24, 25]. In the standard non-resonant production mechanism (small lepton number of the order of baryon number, $L \sim 10^{-10}$) sterile neutrinos are produced via small mixing angle oscillation conversion of thermal active neutrinos [26].

Sterile neutrino with the mass in keV range has a radiative decay channel emitting a photon with an energy that is half of its mass eigenstate. The width of the decay line increases as the fifth power of its mass eigenstate and as square of its mixing angle, being potentially detectable in various X-ray spectra of the astrophysical objects [27, 28]. The strategy to search for dark matter particles possessing a radiative decay channel and to derive the constraints on their parameters from X-ray observations applied to sterile neutrino is discussed in Ref.[29, 30].

The analysis of the observed X-ray background from HEAO-1 and XMM-Newton [31] leads to an upper mass limit for sterile neutrino of $m_{\nu_s} < 8.9$ keV || improved to $m_{\nu_s} < 6.3$ keV from the combined analysis of XMM-Newton observations of the Virgo and Coma clusters [32]. Also, the constraints on the rate of sterile neutrino radiative decay obtained from the analysis of the diffuse X-ray spectrum of Andromeda galaxy leads to $m_{\nu_s} < 3.5$ keV, which is a significant improvement over previous upper limits [33].

Although prone to uncertainties due to the estimate of DM distribution in dwarf galaxy [34], interesting constraints on the parameters of radiative DM decay are obtained from XMM-Newton observations of the DM halo of the Milky Way and Ursa Minor [36]. The recent spectral analysis of the unresolved component of the cosmic X-Ray background in the CHANDRA North and South Deep Fields provides limits on the sterile neutrino mass [37]. The highest Milky Way halo mass estimate provides a limit on sterile neutrino mass of $m_{\nu_s} < 2.9$ keV in Dodelson-Widrow production model [22], while the lowest halo mass estimates provides a more conservative limit of $m_{\nu_s} < 5.7$ keV.

The radiative decay of the sterile neutrino can also augment the ionization fraction of the primordial gas at high redshifts leading to the increase of the temperature of the primordial gas, the enhancement molecular hydrogen formation and of the star formation rate [38, 39, 40].

The combined analysis of the Ly α forest power spectrum measured by SDSS, the CMB anisotropy and the galaxy clustering power spectra yielded to the lower limits for sterile neutrino mass, $m_{\nu_s} > 14$ keV [41] and $m_{\nu_s} > 10$ keV [42] in Dodelson-Widrow production model [22], excluding sterile neutrino as DM candidate. However, the method based on the combined analysis of angular power spectra gives direct limits for the free streaming lengths of DM particles, the limits on their masses depending on their momentum distribution functions and therefore on their production mechanisms.

|| Throughout the paper the sterile neutrino mass is quoted at 95% CL.

Taking into account the deviations from the thermal spectrum of DM particles produced due to the variation of the number of degrees of freedom leading to changes in the time-temperature relation of the primordial plasma and the modification of the neutrino thermal potential [24, 26, 43], the combination of CMB, LSS and Ly α forest angular power spectra leads to $m_{\nu_s} > 1.7$ keV with a further improvement to $m_{\nu_s} > 3$ keV when high-resolution Ly α forest power spectra are considered [43].

In this paper we explore an alternative method to constrain the sterile neutrino mass based on the CMB weak lensing extraction. Distortions of CMB temperature and polarization maps caused by the gravitational lensing potential, observable with high angular resolution and sensitivity, have impact on cosmological parameter degeneracies when non-minimal cosmological scenarios are considered [44, 45, 46, 47].

The CMB weak lensing offers several advantages against the method based on the combination of angular power spectra. As the gravitational lensing effect depends on the dark matter distribution in the Universe, no assumption on light-to-mass bias is required. The projected gravitational potential is sensitive to the matter distribution out to high redshifts, preventing from non-linear corrections required only at very small scales. In addition, unlike the galaxy clustering and the Ly α forest, the projected gravitational potential probes a larger range of angular scales, most of the signature coming from large scales.

The paper is organized as follows. In Section 1 we compute the energy density evolution of the dark matter sterile neutrino in the expanding Universe, incorporating the time-temperature relation and the modification of the neutrino thermal potential. In Section 2 we compute the deflection angle power spectrum and its cross-correlation with the temperature when sterile neutrino dark matter energy density is considered. In Section 3 we derive limits on the sterile neutrino mass from PLANCK weak lensing extraction. We draw our main conclusions in Section 4.

Throughout we assume a background cosmology consistent with the most recent cosmological measurements [3] with energy density of $\Omega_m = 0.3$ in matter, $\Omega_b = 0.05$ in baryons, $\Omega_\nu = 0.01$ in three active neutrino flavors, $\Omega_\Lambda = 0.7$ in cosmological constant, a Hubble constant of $H_0=72$ km s $^{-1}$ Mpc $^{-1}$, a reionization redshift $z_{re}=13$ (assuming a sharp reionization history) and adiabatic initial conditions with a power-law scalar spectral index $n_s = 1$.

1. Sterile neutrino dark matter production and density evolution

1.1. Non-resonant production

Sterile neutrinos dark matter candidates are produced in the early Universe through oscillation with active neutrinos, at temperatures close to QCD phase transition [24, 26]. The oscillation process takes place due to the fact that the neutrino mass eigenstate components propagate differently as they have different energies, momenta and masses. Eigenstates of neutrino interaction include the active neutrinos, ν_a ($a=e, \mu, \tau$), which

are created and destroyed in the standard model by weak interactions as well as the sterile neutrinos, ν_s , which do not participate in weak interactions. For oscillations occurring in vacuum between two neutrino flavors ν_a and ν_s , the mixing can be written as:

$$\begin{aligned} |\nu_a \rangle &= \cos \theta_0 |\nu_1 \rangle + \sin \theta_0 |\nu_2 \rangle \\ |\nu_s \rangle &= -\sin \theta_0 |\nu_1 \rangle + \cos \theta_0 |\nu_2 \rangle, \end{aligned} \quad (1)$$

where ν_1 and ν_2 are the neutrino mass eigenstate components and θ_0 is the vacuum mixing angle. The mixing of antineutrinos can be obtained from the above equation by performing the transformation $\nu_a \rightarrow \bar{\nu}_a$ and $\nu_s \rightarrow \bar{\nu}_s$. It is usual to consider that each neutrino/antineutrino of a definite flavor is dominantly one mass eigenstate. In this circumstance we refer to the dominant mass eigenstate component of $\nu_a/\bar{\nu}_a$ as ν_1 to that of $\nu_s/\bar{\nu}_s$ as ν_2 and to their difference of squared masses as $\delta m^2 = m_{\nu_s}^2 - m_{\nu_a}^2$.

The mixing of the mass eigenstate components are modified in the presence of the finite temperature background either in the case of small active neutrino lepton number, $L_{\nu_a} \sim 10^{-10}$ (of the order of baryon number), driving non-resonant sterile neutrino production [22], or in the case of several orders of magnitude larger lepton number [24, 48]. The lepton number is defined as the difference between the active neutrino and antineutrino number densities normalized by the photon number density: $L_{\nu_a} = (n_{\nu_a} - n_{\bar{\nu}_a})/n_\gamma$.

The matter mixing angle, θ_M , is related to the vacuum mixing angle, θ_0 , through (see e.g. Ref. [24] and references therein):

$$\sin^2 2\theta_M = \frac{\Delta^2(p) \sin^2 2\theta_0}{\Delta^2(p) \sin^2 2\theta_0 + D^2(p) + [\Delta(p) \cos 2\theta_0 + V^L - V^T(p)]^2}. \quad (2)$$

In the above equation $\Delta(p) = \delta m^2/2p$ is the vacuum oscillation factor, V^L is the asymmetric lepton potential, $V^T(p)$ is the thermal potential, $D(p) = \Gamma_{\nu_a}(p)/2$ is the quantum damping rate and Γ_{ν_a} is the collision rate defined as:

$$\Gamma_{\nu_a}(p, T) \approx \begin{cases} 1.27 G_F^2 p T^4, & a = e \\ 0.92 G_F^2 p T^4, & a = \mu, \tau \end{cases}$$

The asymmetric lepton potential, V^L , and the thermal potential $V^T(p)$ read as [24, 26]:

$$\begin{aligned} V^L &= \sqrt{2} G_F \left[2(n_{\nu_a} - n_{\bar{\nu}_a}) + \sum_{a \neq a'} (n_{\nu_{a'}} - n_{\bar{\nu}_{a'}}) - \frac{n_n}{2} \right], \\ V^T &= -\frac{8\sqrt{2} G_F p}{3m_Z^2} (\langle E_{\nu_a} \rangle n_{\nu_a} + \langle E_{\bar{\nu}_a} \rangle n_{\bar{\nu}_a}) \\ &\quad - \frac{8\sqrt{2} G_F p}{3m_W^2} (\langle E_{\nu_a} \rangle n_{\nu_a} + \langle E_{\bar{\nu}_a} \rangle n_{\bar{\nu}_a}), \end{aligned} \quad (3)$$

where: E_{ν_a} is the active neutrino total energy, $n_{\nu_a}/n_{\bar{\nu}_a}$ are neutrino/antineutrino number densities, cosmological n_n is the baryon number density, m_Z is Z^0 boson mass and m_W

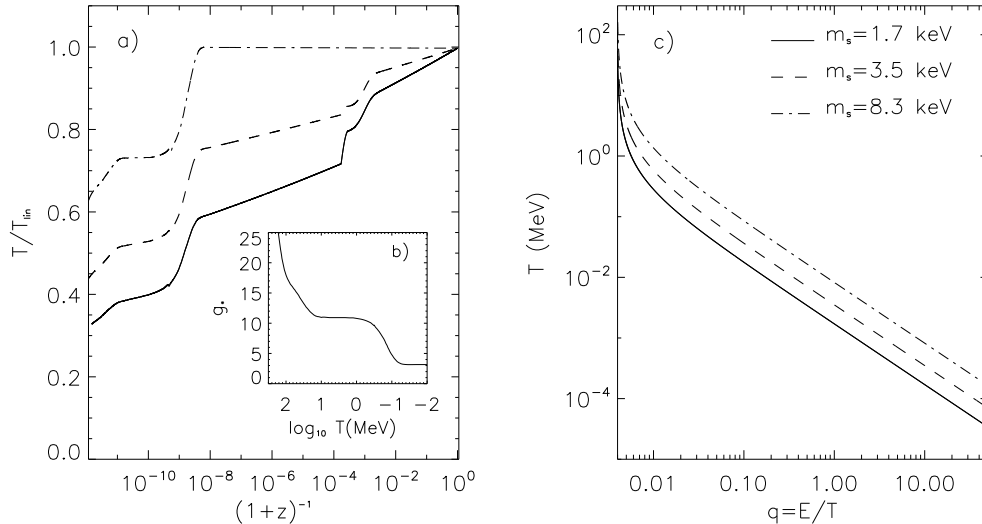


Figure 1. Panel a): The evolution with the scale factor of the temperature obtained by the integration of the time-temperature relation considering the variation of the statistical weight in relativistic particles g^* , compared with the linear evolution of the temperature, $T_{lin} = T_{CMB}(1+z)$. Panel b): The evolution with the temperature of the statistical weight in relativistic particles g^* used in the computation of the time-temperature relation. Panel c): The temperature dependence on sterile neutrino comoving momentum obtained for the same sterile neutrino mass values as in Panel a).

is W^\pm boson mass. The number density of the thermally distributed active neutrinos, n_{ν_a} is given by:

$$n_{\nu_a} = \frac{3}{8} n_\gamma \left(\frac{T_{\nu_a}}{T_\gamma} \right)^3, \quad (4)$$

where $n_\gamma = 2\zeta(3)T_\gamma^3/\pi^2$ is the photon number density and $\zeta(3)$ is the Riemann zeta function of 3.

Throughout we will consider a lepton symmetric Universe ($n_{\nu_a} \simeq n_{\bar{\nu}_a}$) and neglect the contribution to the asymmetric potential due to the baryon number which is very small at the temperatures of interest [26]. In this case the contribution of asymmetric lepton potential V^L in eq. (2) is negligible.

1.2. Energy density evolution

Since sterile neutrinos/antineutrinos are produced non-thermally, their mean energy density and pressure must be computed by the direct integration of their phase-space

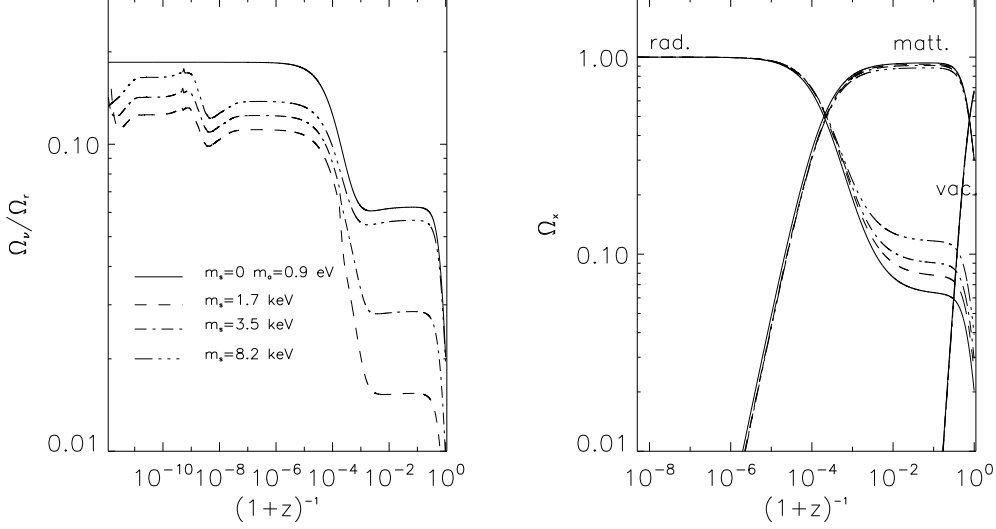


Figure 2. Left: The dependence on the scale factor of the energy density parameters of sterile neutrinos expressed in units of the mean energy density of one mass eigenstate of massless neutrinos for different sterile neutrino mass values. Right: The evolution with the scale factor of the energy density parameters for matter, radiation and vacuum obtained for fiducial model when the corresponding sterile neutrino energy density parameters are included.

distributions:

$$\begin{aligned} \rho_{\nu_s} + \rho_{\bar{\nu}_s} &= \frac{T^4}{2\pi^2} \int_0^\infty dq q^2 E_{\nu_s} [f_{\nu_s}(q) + f_{\bar{\nu}_s}(q)], \\ p_{\nu_s} + p_{\bar{\nu}_s} &= \frac{T^4}{2\pi^2} \int_0^\infty dq \frac{q^2}{E_{\nu_s}} [f_{\nu_s}(q) + f_{\bar{\nu}_s}(q)], \end{aligned} \quad (5)$$

where: f_{ν_s} and $f_{\bar{\nu}_s}$ are the neutrino/antineutrino phase-space distribution functions and $E_{\nu_s} = \sqrt{q^2 + a^2 m_{\nu_s}^2}$ is the total energy of sterile neutrino having a mass m_{ν_s} and a comoving momentum $q = E/T$; $a = (1+z)^{-1}$ is the scale factor ($a_0=1$ today). The temporal evolution of sterile neutrino energy density affects the Hubble expansion rate that reads as:

$$H(a) = \sqrt{\frac{8\pi G}{3}} [\Omega_m/a^3 + \Omega_r/a^4 + \Omega_\Lambda]^{1/2}. \quad (6)$$

In the above equation G is the gravitational constant, $\Omega_m = \Omega_b + \Omega_{cdm} + \Omega_{\nu_a} + \Omega_{\nu_s}$ is the matter energy density parameter where Ω_b , Ω_{cdm} , Ω_{ν_a} and Ω_{ν_s} are the energy density parameters for baryons, cold dark matter, active and sterile neutrinos respectively, Ω_r is the radiation energy density parameter and Ω_Λ is the vacuum energy density parameter.

Depending on the mass, the maximum rate production of sterile neutrino occurs at [22, 49]:

$$T_{max} \approx 133 \text{ MeV} \left(\frac{m_{\nu_s}}{1 \text{ keV}} \right)^{1/3}.$$

For sterile neutrino with mass in the range of interest, the time evolution of the temperature-dependent thermal potential and of the collision rate require the knowledge of the time-temperature relation in the expanding Universe:

$$\frac{da}{dT} = \frac{d\rho_{tot}}{dT} (\rho_{tot} + p_{tot})^{-1}, \quad (7)$$

where ρ_{tot} and p_{tot} are the total density and pressure, including the contribution of sterile neutrino/antineutrino as given in equation (5). The time-temperature relation takes into account the variation of statistical weight in relativistic particles that is changed by nearly an order of magnitude since T_{max} [24, 43]. A general treatment of the time-temperature relation, whose approach we have incorporated, is given in the Appendix of Ref. [24].

Left panel of Figure 1 presents the evolution with the scale factor of the temperature obtained by the intergration of the time-temperature relation taking into account the variation of the statistical weight in relativistic particles g^* , compared with the linear evolution of the temperature $T_{lin} = T_{CMB}(1+z)$. We also show, in the right panel of the same figure, the dependence of the temperature on sterile neutrino comoving momentum.

The time evolution of the sterile neutrino phase-space distribution, f_{ν_s} , can be described by the semiclassical Boltzmann equation [22, 24]:

$$\frac{\partial}{\partial t} f_{\nu_s}(q) - H(t) q \frac{\partial}{\partial q} f_{\nu_s}(q) \approx \Gamma(\nu_a \rightleftharpoons \nu_s) [f_{\nu_a}(q) - f_{\nu_s}(q)], \quad (8)$$

where: $dt = da/aH(a)$, f_{ν_a} is the active neutrino phase-space distribution and $\Gamma(\nu_a \rightleftharpoons \nu_s)$ is the effective production/annihilation rate of sterile neutrinos:

$$\Gamma(\nu_a \rightleftharpoons \nu_s) \approx 0.25 \Gamma_{\nu_a}(p, T) \sin^2 2\theta_M. \quad (9)$$

We use the set of equations (5)-(9) to compute the temporal evolution of the energy density of sterile neutrinos in the expanding Universe. For sterile neutrino with the mass in the range of interest, the flavor dependence is almost negligible [26], implying that similar results can be obtained for all $\nu_a \rightleftharpoons \nu_s$ mixings. Throughout we consider $\nu_\tau \rightleftharpoons \nu_s$ mixing.

Left panel of Figure 2 presents the dependence on the scale factor of the energy density parameter of sterile neutrino expressed in units of the mean energy density of one mass eigenstate of massless neutrinos for three different mass values. We also show the same dependence for the case $m_{\nu_s} = 0$. The right panel of the same figure shows the evolution with the scale factor of the energy density parameters for matter, radiation and vacuum obtained for our flat Λ CDM background cosmology when the corresponding sterile neutrino masses are included. The production of DM sterile neutrino affects the radiation and matter evolution through the Hubble expansion rate, altering the time-temperature relation and redshifting the relativistic species.

2. CMB lensing extraction with PLANCK experiment

2.1. Deflection angle power spectrum

The CMB photons from the last scattering surface are subject to the cumulative effects of the large scale structure gravitational potential [50]. The net result is that the CMB temperature anisotropy and polarization patterns measured in the direction \mathbf{n} in the sky provides information on the photons emerging from the last scattering surface from the direction $\tilde{\mathbf{n}} = \mathbf{n} + \delta\mathbf{n}$. The intensity and the linear polarization of the lensed CMB are completely specified by the Stokes parameters I , Q and U which are related with the unlensed Stokes parameters through: $X(\mathbf{n}) = \tilde{X}(\tilde{\mathbf{n}})$, where $X(\mathbf{n})$ stands for the lensed I , Q and U . The deflection field is defined as the gradient of the lensing potential $\delta\mathbf{n} = \nabla\Psi(\mathbf{n})$, where ∇ is the covariant derivative on the sphere.

The deflection map and the lensing potential map can be expanded in spherical harmonics [51, 52], so that the relation between the deflection angle power spectrum C_l^{dd} and the lensing potential power spectrum $C_l^{\Psi\Psi}$ is given by [53]:

$$C_l^{dd} = l(l+1)C_l^{\Psi\Psi}. \quad (10)$$

The power spectra of the lensing potential, $C_l^{\Psi\Psi}$ and the correlation with the temperature anisotropy, $C_l^{\Psi T}$, can be numerically computed by using the Code for Anisotropies in the Microwave Background (CAMB) [50, 52, 54] in the linear theory as well as by including the non-linear corrections from HALOFIT [55]. We recall that $C_l^{\Psi T}$ does not vanish because the temperature map includes information on the time variation of the gravitational potential through the integrated Sachs-Wolfe effect.

We modified the CMB anisotropy code CAMB to compute the CMB angular power spectra in the presence of a DM sterile neutrino component. We include in the computation the momentum-dependent sterile neutrino phase-space distribution function, as described in the previous section, its unperturbed and perturbed energy density and pressure, energy flux and shear stress.

Figure 3 presents in the top panel the deflection angle power spectrum, C_l^{dd} , obtained in our fiducial model ($m\nu_s = 0$). The bottom panel of Figure 3 shows the relative percentual differences between the fiducial model and exact the same model but with $m\nu_s = 1.7, 3.5$ and 8.3 keV.

The signature of sterile neutrino mass on the deflection angle power spectrum is the suppression of its amplitude relative to the fiducial model. The net suppression is scale dependent and the relevant length scale is the free-streaming scale [56], which increases with the mean dark matter sterile neutrino velocity and decreases with its mass.

3. Constraints on sterile neutrino mass from PLANCK lensing extraction

3.1. Gaussian Likelihood function

In the standard inflationary cosmology, the spherical harmonic coefficients of the unlensed temperature and polarization field in the sky obey the Gaussian statistics

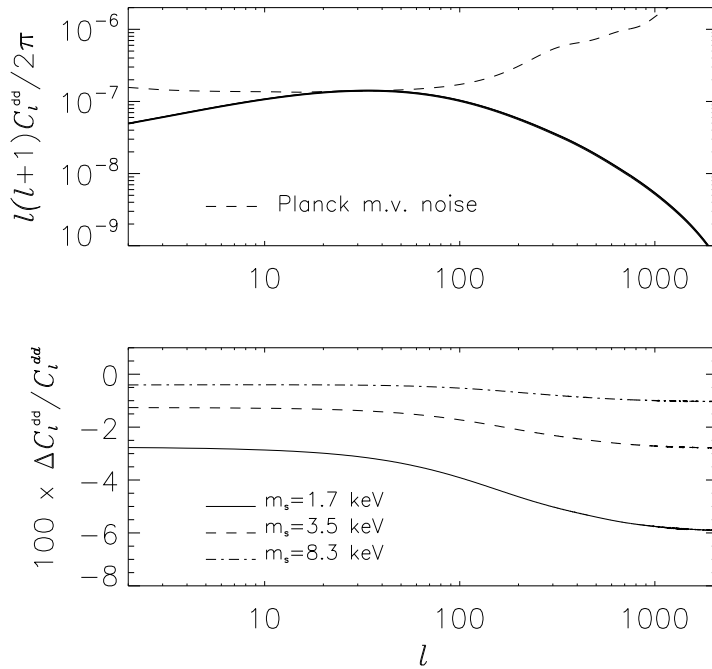


Figure 3. Top panel: The deflection angle power spectrum, C_l^{dd} , obtained in the our fiducial model ($m_{\nu_s} = 0$) and the minimum variance noise power spectrum (dashed line) for PLANCK experimental characteristics given in Table 1. Bottom panel: The relative percentual differences between the fiducial model ($m_{\nu_s} = 0$) and exactly the same model with $m_{\nu_s} = 1.7, 3.5$ and 8.3 keV.

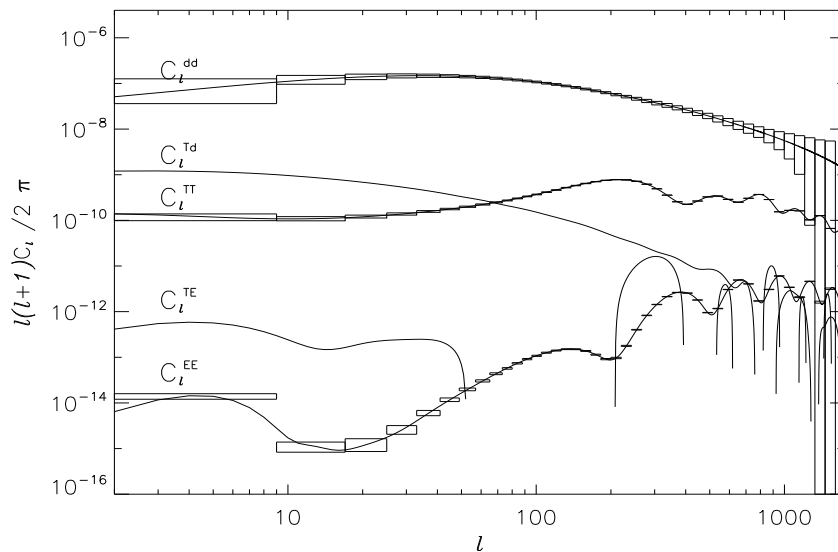


Figure 4. The CMB angular power spectra for the fiducial model. The error bars include the Planck experiment instrumental noise and the cosmic variance. For graphical representation convenience, the error bars assume a multipole binning of $\Delta l = 7$ until $l \sim 70$ and then $\Delta l \sim l/10$ [61, 63].

and can be used to define the estimators of the covariance:

$$\hat{C}_l^{ab} = \frac{1}{2l+1} \sum_m W_{lm}^* X_{lm} \quad a, b \in \{T, E, B\}, \quad (11)$$

where W_{lm} and X_{lm} are the harmonic coefficients of the CMB temperature and polarization anisotropy maps. The corresponding full-sky likelihood function is given by:

$$\chi^2 = -2 \ln \mathcal{L}(\hat{\mathbf{C}}|\mathbf{C}) = (2l+1) \{ \text{Tr}[\hat{\mathbf{C}}\mathbf{C}^{-1}] + \ln |\mathbf{C}| \}, \quad (12)$$

where \mathbf{C} is the covariance matrix of the observations and $\hat{\mathbf{C}}$ is the corresponding covariance matrix of estimators. The covariance matrix of the observations reads as:

$$\mathbf{C} = \begin{pmatrix} \tilde{C}_l^{TT} + N_l^{TT} & \tilde{C}_l^{TE} & 0 \\ \tilde{C}_l^{TE} & \tilde{C}_l^{EE} + N_l^{EE} & 0 \\ 0 & 0 & \tilde{C}_l^{BB} + N_l^{BB} \end{pmatrix}. \quad (13)$$

In the above equation \tilde{C}_l^{ab} , $a, b = \{T, E, B\}$ are the unlensed power spectra of primary anisotropies, N_l^{ab} are the corresponding instrumental noise variances and the parity invariance ($C_l^{BT} = C_l^{BE} = 0$) it is assumed.

Weak lensing correlates the lensed multipoles and the lensed sky is not any more Gaussian [57]. However, as shown in Ref.[58], at least up to PLANCK resolutions and sensitivities, equation (11) remains approximately correct if the B-mode, that is noise dominated, is not included in the covariance matrix. The non-Gaussian corrections can be however important for the future high sensitivity CMB polarization experiments having a signal dominated B-mode power spectrum [59].

In this paper we consider a fiducial model with no significant amplitude of the primordial gravitational waves, omitting the B-mode from the parameter estimation analysis. In this case, the data covariance matrix read as:

$$\mathbf{C} = \begin{pmatrix} C_l^{TT} + N_l^{TT} & C_l^{TE} & C_l^{Td} \\ C_l^{TE} & C_l^{EE} + N_l^{EE} & 0 \\ C_l^{Td} & 0 & C_l^{dd} + N_l^{dd} \end{pmatrix}, \quad (14)$$

where C_l^{ab} , $a, b = \{T, E\}$, are the lensed CMB power spectra, N_l^{ab} are the corresponding detector noise power spectra, C_l^{dd} is deflection angle power spectrum, N_l^{dd} the noise power spectrum associated to the lensing extraction and C_l^{Td} is the power spectrum of the cross-correlation between the temperature and deflection angle.

The weak lensing does not change the total variance in the CMB temperature anisotropy and polarization maps and hence lensed observations have the same variance as if there were no lensing [58, 59].

For each frequency channel we consider an homogeneous detector noise with the power spectrum, $N_{l,\nu}^{ab}$, given by [60]:

$$N_{l,\nu}^{ab} = (\theta_b \Delta_c)^2 \exp^{l(l+1)\theta_b^2/8 \ln 2}, \quad (15)$$

Table 1. The expected experimental characteristics for the PLANCK frequency channels considered in this work [61]: ν is the frequency of the channel, θ_b is the FWHM, Δ_T and Δ_P are the sensitivities per pixel for temperature and polarization maps.

ν (GHz)	FWHM (arc-minutes)	Δ_T (μ K)	Δ_P (μ K)
100	9.5	6.8	10.9
143	7.1	6.0	11.4
217	5.0	13.1	26.7

where ν is the frequency of the channel, θ_b is the FWHM of the beam and Δ_c , where $c \in (T, P)$, are the sensitivities per pixel for the temperature and polarization maps. The global noise of the experiment, N_l^{XX} , can be written as:

$$N_l^{ab} = \left[\sum_{\nu} (N_{l,\nu}^{ab})^{-1} \right]^{-1}. \quad (16)$$

The expected experimental performances of the PLANCK frequency channels considered in this paper [61] are presented in Table 1.

The lensing noise power spectrum, N_l^{dd} , was numerically computed by using the minimum variance quadratic estimator of Okamoto and Hu [62]. By definition, the quadratic estimator is build from pairs (a, b) of observed temperature or polarization modes and its multipoles are given in the quadratic form:

$$d(a, b)_L^M = N_L^{ab} \sum_{ll'mm'} \mathcal{G}(a, b)_{ll'}^{mm'} a_l^m b_{l'}^{m'}, \quad (17)$$

where a_l^m and b_l^m correspond to the lensed CMB fields. The minimum variance estimator is obtained by finding the weights $\mathcal{G}_{l_1 l_2}^{a, b}(L)$ that minimize the Gaussian variance:

$$\langle d(a, b)_L^{M*} d(a', b')_L^M \rangle \equiv \delta_{L, L'} \delta_{M, M'} [C_L^{dd} + \mathcal{N}_L^{aba'b'}]. \quad (18)$$

For the minimum variance estimator the lensing noise reads as:

$$N_l^{dd} = \left[\sum_{aba'b'} (\mathcal{N}^{aba'b'})^{-1} \right]^{-1}. \quad (19)$$

In the top panel of Figure 3 we show the lensing noise power spectrum, N_l^{dd} , for PLANCK experiment, obtained by using the minimum variance estimator method.

Figure 4 presents the CMB angular power spectra for the fiducial model. The error bars, ΔC_l^α , include the instrumental noise and the cosmic variance:

$$\Delta C_l^\alpha = \sqrt{\frac{2}{(2l+1)\Delta l f_{sky}}} (C_l^\alpha + N_l^\alpha) \quad \alpha = [TT, EE, TE, dd, Td]. \quad (20)$$

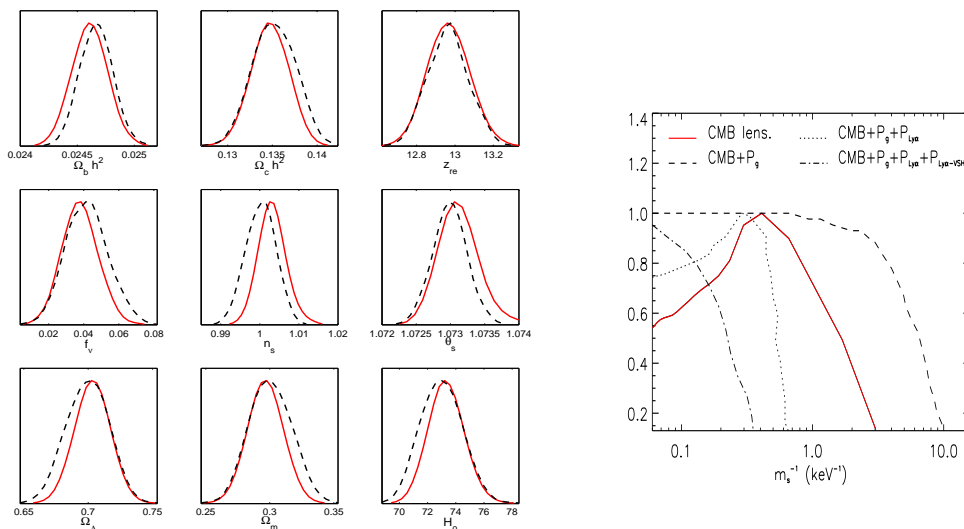


Figure 5. Left: The marginalized likelihood probabilities for PLANCK-like observations obtained by using the lensing extraction with (solid red line) and without (dashed black line) DM sterile neutrino component. Right: The marginalized likelihood probabilities for the (inverse) mass of DM sterile neutrino obtained for the PLANCK-like observations with lensing extraction (solid red line) compared with the marginalized likelihoods obtained from [43]: CMB plus SDSS 3D power spectrum (dashed line), plus SDSS Ly α forest power spectrum (dotted line), plus VHS high-resolution Ly α forest power spectrum (dash-dotted line).

In the above equation f_{sky} represents the fraction of the sky covered by the observations. For the purpose of this work we take $f_{sky}=0.8$ and assume a perfect cleaning of all the astrophysical foregrounds. For graphical representation convenience, the error bars presented in Figure 4 assume a multipole binning of $\Delta l = 7$ until $l \sim 70$ and then $\Delta l \sim l/10$ [61, 63]:

3.2. Parameters estimation

We assume a flat Λ CDM cosmological model with the following set of parameters to be determined from the PLANCK-like observations:

$$\Theta = (\Omega_b h^2, \Omega_c h^2, \theta_s, z_{re}, f_\nu, m_{\nu_s}, n_s)$$

where Ω_b and Ω_c are the fractions of critical density in baryons and cold dark matter, θ_s is the angular acoustic peak scale of the CMB, z_{re} is the reionization redshift (we assume a sharp reionization history), f_ν is the fraction of massive neutrinos, m_{ν_s} is the sterile neutrino mass and n_s is the spectral index of primordial adiabatic perturbations.

We use the COSMOMC [64] Monte Carlo Markov Chain (MCMC) public package with the modification of the function CHISQEXACT [63] required to compute the likelihood function when the deflection angle power spectrum is included, to sample for the posterior distribution of parameters space Θ , giving the PLANCK-like data. For graphical representation convenience, the error bars in Figure 4 assume a multipole binning of $\Delta l = 7$ until $l \sim 70$ and then $\Delta l \sim l/10$ [61, 63]:

Left panel from Figure 5 presents the marginalized likelihood probabilities of the cosmological parameters for PLANCK-like observations obtained from lensing extraction with and without the DM sterile neutrino component, showing that the cosmological parameters are generally not biased when including DM sterile neutrino.

In the right panel of Figure 5 we present the marginalized likelihood probability for the inverse mass, m_s^{-1} , of sterile neutrino obtained for PLANCK-like observations by using the lensing extraction. We find a lower limit on the sterile neutrino dark matter $m_{\nu_s} > 2.08$ keV at 95% CL, in agreement with our previous result [65] obtained from PLANCK lensing extraction by using the Fisher information matrix ($m_{\nu_s} > 1.75$ keV). For comparison we also show in the same figure the marginalized likelihoods for $m_{\nu_s}^{-1}$ obtained in Ref. [43] from: CMB plus SDSS 3D power spectrum, plus SDSS Ly α forest power spectrum, plus VHS high-resolution Ly α forest power spectrum. Our result is in agreement with the result from the combined analysis of CMB, SDSS 3D power spectrum and SDSS Ly α forest power spectrum ($m_{\nu_s} > 1.7$ keV) but is less constrained than the limit obtained when VHS high-resolution Ly α forest data are included ($m_{\nu_s} > 3$ keV).

4. Conclusions

From the future high precision observations of the PLANCK satellite we would like to extract information about both unlensed and lensed CMB anisotropies. The weak lensing effects of the CMB induced by the neighbouring galaxy clustering will have a significant effect on the statistics of the observed CMB and must be taken into account in order to obtain reliable parameter estimates, offering several advantages against the cosmological parameter extraction based on the combination of CMB, LSS and Ly α power spectra. As the gravitational lensing effect depends on the matter distribution, no assumption on light-to-mass bias is required. In addition, unlike the galaxy clustering and Ly α forest power spectra, the projected gravitational potential power spectrum probes a larger range of angular scales, the non-linear corrections being required only on very small scales.

However, the amount of information that can be obtained from the CMB weak lensing extraction depends on the lensing noise level.

In this paper we address the possibility to constrain the DM sterile neutrino mass from PLANCK-like observations by using the CMB lensing extraction. We use the minimum variance estimator of Okamoto and Hu [62] to compute the lensing noise power spectrum for PLANCK experimental configuration.

Taking into account the changes in the time-temperature relation of the primordial plasma and the modification of the neutrino thermal potential, we compute the projected gravitational potential power spectrum and its correlation with the temperature in the presence of DM sterile neutrino component that together with the lensed CMB temperature and polarization anisotropy power spectra are used to constrain the cosmological parameters including sterile neutrino mass, from PLANCK-like observations.

We show that the cosmological parameters are generally not biased when DM sterile neutrino is included. From this analysis we found a lower limit on DM sterile neutrino mass $m_{\nu_s} > 2.08$ keV at 95% CL, consistent with the lower mass limit obtained from the combined analysis of CMB, SDSS 3D power spectrum and SDSS Ly α forest power spectrum ($m_{\nu_s} > 1.7$ keV) [43].

We conclude that, although the information that can be extracted is rather limited due to the high level of the lensing noise of PLANCK experiment, the weak lensing of CMB offers a valuable alternative to constrain the dark matter sterile neutrino mass.

Acknowledgements

We thank to Oleg Ruchayskiy and Alexey Boyarsky for the useful comments. We acknowledge the use of the GRID computing system facility at the Institute for Space Sciences Bucharest and the staff working there.

References

- [1] Hinshaw G et al (WMAP Collaboration), 2007 *Astrophys. J. Suppl.* **170** 288 [astro-ph/0603451]
- [2] Page L et al (WMAP Collaboration), 2007 *Astrophys. J. Suppl.* **170** 335 [astro-ph/0603450]
- [3] Spergel D N et al (WMAP Collaboration), 2007 *Astrophys. J. Suppl.* **170** 377 [astro-ph/0603449]
- [4] Seljak U, Solsar A and McDonald P, 2006 *J. Cosmol. Astropart. Phys.* JCAP10(2006)014 [astro-ph/0604335]
- [5] Turner M S, 2000 *Phys. Rep.* **333** 619 ; Wang X, Tegmark M, and Zaldarriaga M (2002) *Phys. Rev D* **65** 123001 [astro-ph/0105091]; Bachall N A, Ostriker J P, Perlmutter S and Steinhardt P J, 1999 *Science* **284** 1481 [astro-ph/9906463]
- [6] Primack J R, 2001 *Proceedings of the NATO Advanced Study Institute* Kluwer Academic Publishers **34** 349
- [7] Colombi S, Dodelson S and Widrow L M, 1996 *Astrophys. J.* **458** 1 [astro-ph/9505029]
- [8] Bode P, Ostriker J P and Turok N , 2001 *Astrophys. J.* **556** 93 [astro-ph/0010389]
- [9] Padmanabhan T, 1995 *Space science reviews* **73** 436
- [10] Dalcanton J J and Hogan C J, 2001 *Astrophys. J.* **561** 35 [astro-ph/0004381]
- [11] van den Bosch F C and Swaters R A, 2001 *Mon. Not. R. Astron. Soc.* **325** 1017 [astro-ph/0006048]
- [12] Zentner A N and Bullock J S, 2002 *Phys. Rev. D* **66** 043003 [astro-ph/0205216]
- [13] Dolgov A D and Sommer-Larsen J, 2001 *Astrophys. J.* **551**, 608 [astro-ph/9912166]
- [14] Athanassopoulos C et al, 1996 *Phys. Rev. Lett.* **77** 3082 [nucl-ex/9605003]
- [15] Aguilar-Arevalo A A et al (MiniBooNE Collaboration) 2007 [hep-ex/0704.1500]
- [16] Maltoni M. ans Schwets T, 2007 [hep-ex/0705.0107]
- [17] Cirelli M , Marandella G, Strumia S, Vissani F, 2005 *Nucl. Phys. B* **708** 215 [hep-ph/0403158]
- [18] Hannestad S and Raffelt G G, 2006 *J. Cosmol. Astropart. Phys.* JCAP11(2006)016 [astro-ph/0607101]
- [19] Dodelson S, Melchiorri A and Slosar A, 2006 *Phys. Rev. Lett.* **97** 041301 [astro-ph/0511500]
- [20] Kristiansen J, Eriksen H K and Elgary , 2006 *Phys. Rev. D* **74** 123005 [astro-ph/0608017]
- [21] Tremaine S and Gunn J E, 1979 *Phys. Rev. Lett.* **42** 407
- [22] Dodelson S, Widrow L M, 1994 *Phys. Rev. Lett.* **72**, 17 [hep-ph/9303287]
- [23] Dolgov A D and Hansen S H, 2002 *Astropart. Phys.* **16** 339 [hep-ph/0009083]
- [24] Abazajian K, Fuller G M, Patel M, 2001 *Phys. Rev. D* **64** 023501 [astro-ph/0101524]
- [25] Asaka T, Sahaposhnikov M and Kusenko A, 2006 *Phys. Lett. B* **638** 401 [hep-ph/0602150]
- [26] Abazajian K N and Fuller G M, 2002 *Phys. Rev. D* **66** 023526 [astro-ph/0204293]

- [27] Pal P B and Wolfenstein L, 1982 *Phys. Rev.* **D 25**, 766
- [28] Abazajian K, Fuller G M and Tucker W H, 2001 *Astrophys. J.* **562** 593 [astro-ph/0106002]
- [29] Boyarsky A, Neronov A, Ruchayskiy O, Shaposhnikov M, Tkachev I, 2006 *Phys. Rev. Lett.* **97** 261302 [astro-ph/0603660]
- [30] Riemer-Srensen S, Hansen S H, Pedersen K, 2006 *Astrophys. J.* **644** L33 [astro-ph/0603661]
- [31] Boyarsky A, Neronov A, Ruchayskiy O and Shaposhnikov M, 2006 *Mon. Not. R. Astron. Soc.* **370** 213 [astro-ph/0512509]
- [32] Boyarsky A, Neronov A, Ruchayskiy O and Shaposhnikov M, 2006 *Phys. Rev* **D 74** 103506 [astro-ph/0603368]
- [33] Watson C R, Beacom J F, Yüksel H, Walker T, 2006 *Phys. Rev.* **D 74** 033009 [astro-ph/0605424]
- [34] Abazajian K and Koushiappas S, 2006 *Phys. Rev.* **D 74** 023527 [astro-ph/0605271]
- [35] Abazajian K, Fuller G M, Tucker W H, 2001 *Astrophys. J.* **562** 593 [astro-ph/0106002]
- [36] Boyarsky A, Nevalainen J, Ruchayskiy O, 2007 *Astron. Astrophys.* **471** 51 [astro-ph/0610961]
- [37] K. Abazajian, M. Markevitch, S. M. Koushiappas, R. C. Hickox, 2007 *Phys. Rev.* **D 75** 063511 [astro-ph/0611144]
- [38] Biermann P L and Kusenko A, 2006 *Phys. Rev. Lett.* **96** 091301 [astro-ph/0601004]
- [39] Ripamonti E, Mapelli M and Ferrara A, 2007 *Mon. Not. R. Astron. Soc.* **375**, 1399 [astro-ph/0606483]
- [40] Mapelli M, Ferrara A and Perpaoli E, 2006 *Mon. Not. R. Astron. Soc.* **369** 1719 [astro-ph/0603237]
- [41] Seljak U, Makarov A, McDonald P, Trac H, 2006 *Phys. Rev. Lett.* **97** 191303 [astro-ph/0602430]
- [42] Viel M, Lesgourgues J, Haehnelt M G, S. Matarrese, A. Riotto, 2006 *Phys. Rev. Lett.* **97**, 071301 [astro-ph/0605706]
- [43] Abazajian K, 2006 *Phys. Rev.* **D 73**, 063513 [astro-ph/0512631]
- [44] Abazajian K and Dodelson S, 2003 *Phys. Rev. Lett.* **91** 041301 [astro-ph/0212216]
- [45] Kaplinghat M, Knox L, Song Y S, 2003 *Phys. Rev. Lett.* **91** 241301 [astro-ph/0303344]
- [46] Lesgourgues J, Perotto L, Pastor S, Piat M, 2006 *Phys. Rev* **D 73** 045021 [astro-ph/0511735]
- [47] Seljak, U and Zaldarriaga M, 1998 *Phys. Rev.* **D 60** 15 [astro-ph/9811123]
- [48] Shi X and Fuller G M, 1999 *Phys. Rev. Lett.* **82** 2832 [astro-ph/9810076]
- [49] Barbieri R and Dolgov A D, 1990 *Phys. Lett.* **B 237** 440 ; Kainulainen K, 1990 *Phys. Lett.* **B244** 191
- [50] Hu W, 2000 *Phys. Rev.* **D 62** 043007 [astro-ph/0002238]
- [51] Hirata C M and Seljak U, 2003 *Phys. Rev.* **D 68** 083002 [astro-ph/0306354]
- [52] Challinor A and Lewis A, 2005 *Phys. Rev.* **D 71** 103010 [astro-ph/0502425]
- [53] Hu W and Okamoto T, 2002 *Astrophys. J.* **574** 566 [astro-ph/0111606]
- [54] Lewis A, Challinor A and Lasenby A, 2000 *Astrophys. J.* **538** 473 [astro-ph/9911177] ¶
- [55] Smith R E et al., 2003 *Mon. Not. R. Astron. Soc.* **341** 1311 [astro-ph/0207664]
- [56] Bond J R and Szalay A S, 1983 **274** 443; Ma C, 1996 *Astrophys. J* **471** 13; Hu W and Eisenstein D J, 1998 *Astrophys. J* **498** 497
- [57] Seljak U, 1996 *Astrophys. J* **463** 1 [astro-ph/9505109]
- [58] Lewis A, 2005 *Phys. Rev.* **D 71** 3008 [astro-ph/0502469]
- [59] Smith K M, Hu W and Kaplinghat M, 2004 *Phys. Rev* **D 70** 3002 [astro-ph/0402442]
- [60] Knox L, 1995 *Phys. Rev.* **D 52** 4307 [astro-ph/9504054]
- [61] The PLANCK Consortia, 2005 "The Scientific Programme of PLANCK" *ESA-SCI* 1 [astro-ph/0604069]
- [62] Okamoto T and Hu W, 2003 *Phys. Rev.* **D 67** 083002 [astro-ph/0301031]
- [63] Perotto L, Lesgourgues J, Hannestad S, Tu H, Wong Y, 2006 *J. Cosmol. Astropart. Phys.* JCAP10(2006)013 [astro-ph/0606227] +
- [64] Lewis A and Bridle S, 2002 *Phys. Rev.* **D 66** 103511 [astro-ph/0205436] *

¶ <http://camb.info>+ <http://lappweb.in2p3.fr/perotto/FUTURCMB>* <http://cosmologist.info/cosmomc>

[65] Popa, L A and Vasile A, 2007 [astro-ph/0701331]